

CLASSIFICATION OF LOW BACKSCATTER OCEAN REGIONS USING LOG-CUMULANTS

Stine Skrunes and Camilla Brekke

Department of Physics and Technology, UiT - The Arctic University of Norway
E-mail: stine.skrunes@uit.no, camilla.brekke@uit.no

ABSTRACT

In a synthetic aperture radar image, low backscatter regions of various origin can be observed in ocean areas. Operational oil spill detection services work to discriminate anthropogenic oil spills from natural phenomena such as seeps, low wind fields, thin ice and biogenic slicks. In this paper, we investigate the potential of using matrix log-cumulants for this purpose.

Key words: SAR, oil spill, look-alikes, log-cumulants, statistics, characterization.

1. INTRODUCTION

Oil is released into the world's oceans on a regular basis. Large scale accidents that take place during oil production and transportation receive much attention from the public and the media. However, large quantities of oil are also released during smaller but frequent operational discharges from ships, that are intentional and often illegal. Satellite synthetic aperture radar (SAR) is an effective tool for detection of oil spills. A review on oil spill observation by SAR can be found in [1]. One of the main challenges for oil spill detection by SAR is natural phenomena that produce similar SAR signatures as oil spills. These are called *look-alikes* and include low wind regions, grease ice, rain cells and biogenic surface slicks. Traditionally, features related to region geometry, characteristics of the backscatter levels, contextual information and spatial texture have been used to classify possible oil spills [2]. Over the last decade, a potential for using multipolarization techniques for discrimination between oil spills and other phenomena has been demonstrated, see, e.g., [3, 4, 5]. In [6] and [7], log-cumulants (defined in [8, translated in [9]] and [10]) were investigated for the purpose of oil versus look-alike discrimination.

The objective of this paper is to further evaluate the potential for classification of low backscatter ocean regions using first and second order log-cumulants.

2. LOG-CUMULANTS

Low backscatter regions of various origin are here compared in terms of log-cumulants, which provide information on statistical properties of the data.

2.1. Theory

According to the *product model*, radar measurements can be expressed as a product of two separate processes, i.e., *speckle* (see, e.g., [11]) and *texture*. The latter refers to the variation in the underlying radar cross section. The presence of texture, and its properties, can be investigated by evaluating log-cumulants, which are cumulants in the log-domain.

Previous work has shown that for cross-polarization channels, a large part of the signal values lies below the sensor noise floor [5]. Therefore we have chosen to discard these channels, and work only on dual-copolarization measurements, i.e., HH and VV channels. The log-cumulants are hence computed from the 2×2 dual-copolarization covariance matrix (which is a submatrix of the original 3×3 matrix), given as

$$\mathbf{C} = \begin{bmatrix} \langle |S_{HH}|^2 \rangle & \langle S_{HH} S_{VV}^* \rangle \\ \langle S_{VV} S_{HH}^* \rangle & \langle |S_{VV}|^2 \rangle \end{bmatrix}. \quad (1)$$

The resulting sample *matrix log-cumulants* (MLCs) of first and second order represent the mean and variance in the log-domain, respectively, and are given by [10]

$$\kappa_1\{\mathbf{C}\} = \mu_1\{\mathbf{C}\}, \quad (2)$$

$$\kappa_2\{\mathbf{C}\} = \mu_2\{\mathbf{C}\} - \mu_1\{\mathbf{C}\}^2, \quad (3)$$

where μ_ν is the *matrix log-moment* of order ν for a set of N samples, defined as

$$\mu_\nu\{\mathbf{C}\} = \frac{1}{N} \sum_{i=1}^N (\ln|\mathbf{C}_i|)^\nu. \quad (4)$$

For further information on log-cumulants, the reader is referred to [8, translated in [9]] and [10].

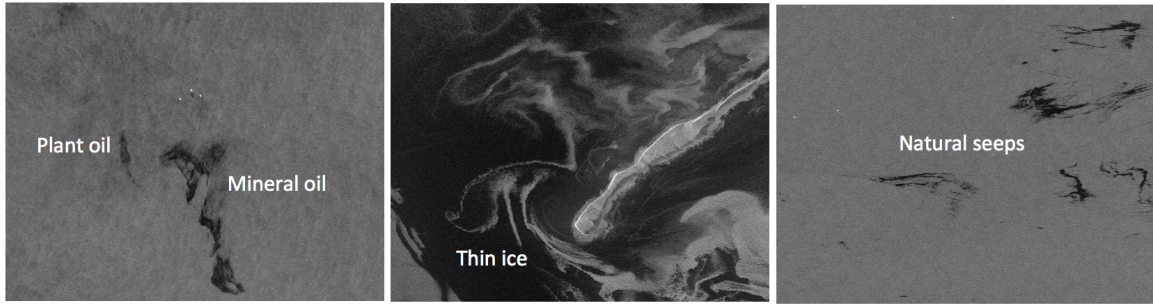


Figure 1: Examples of Radarsat-2 scenes containing low backscatter regions of various origin. Left: experimental releases during an oil-on-water exercise in the North Sea. Middle: thin ice close to Hopen in the Barents Sea. Right: natural seeps in the Gulf of Mexico. RADARSAT-2 Data and Products ©MDA LTD. (2012/2014/2011) - All Rights Reserved.

2.2. Oil Spill Application

In [6] and [7], log-cumulants were investigated for the purpose of oil versus look-alike discrimination. First results presented in [6] examined the second and third order log-cumulants calculated from single-look VV intensity data. Promising results for discriminating mineral oil spills from simulated biogenic slicks and a natural phenomenon were found for both Radarsat-2 and TerraSAR-X data, particularly for κ_2 . The study was expanded to the multipolarization case in [7]. In that paper, log-cumulants of first and second order were extracted from multilooked dual-copolarization data. A separation between mineral oil slicks and other low backscatter phenomena was found in the log-cumulant space. The log-cumulants were normalized with respect to water to account for variation between scenes, e.g., due to varying incidence angle and wind conditions. These are denoted $\tilde{\kappa}_1$ and $\tilde{\kappa}_2$. The results in [7] indicated that mineral oils are characterized by low values of $\tilde{\kappa}_1$ and large values of $\tilde{\kappa}_2$, compared to clean sea and other low backscatter regions. The former reflects the reduced backscatter from these areas compared to clean sea due to wave damping (and possibly a reduction in the dielectric constant). The large values of $\tilde{\kappa}_2$ may indicate a larger internal variation (more radar texture) in mineral oils compared to clean sea and look-alikes. Inhomogeneous distribution of oil may cause this behavior. The natural phenomena were characterized by larger $\tilde{\kappa}_1$, i.e., less signal damping, and lower $\tilde{\kappa}_2$, indicating less texture or more homogeneous regions. In [7], a potential future application of the method for classification of low backscatter regions of unknown origin was suggested. However, the need for further investigations on a larger data set was emphasized.

3. DATA SET

This study is based on data collected by Radarsat-2 in the fine quad-polarization mode. The data were collected from two main geographical regions, i.e., i) the North Sea and the Barents Sea, and ii) the Gulf of Mexico. The data set from the North Sea and Barents Sea contains a ship release, natural low backscatter regions (low wind and/or

Table 1: Number of scenes and ROIs in the data set (in total, and for scenes with incidence angles (θ) below 40° only). Regions are divided into four classes, i.e., natural phenomena (N), mineral oil spills (O), plant oil, used for simulation of biogenic slicks (P), and natural seeps (S).

	North Sea /Barents Sea	Gulf of Mexico
No. of scenes	8	14
	O (9), N (4), P (4)	O (9), S (24)
No. of scenes, $\theta < 40^\circ$	6	5
	O (7), N (4), P (3)	O (6), S (9)

thin ice) and experimental releases of mineral oil and plant oil. The latter substance was released to simulate a natural biogenic slick (see [5] for more information). In the Gulf of Mexico, natural seeps and anthropogenic oil releases, including ship releases and the Deepwater Horizon (DWH) oil spill in 2010, were imaged. Table 1 gives an overview of the data set, with the number of scenes and regions of interest (ROIs) of various types. Some examples are shown in Fig. 1.

4. RESULTS

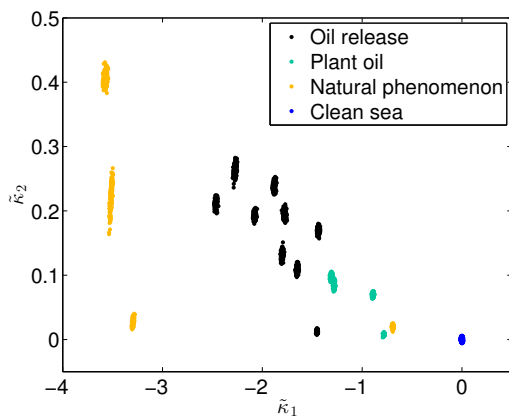
For each scene, the ROIs were segmented, and the log-cumulants were calculated based on a random sample of 4000 pixels. The computation was repeated 200 times for each segment. The resulting normalized log-cumulants were plotted into the $\tilde{\kappa}_1 - \tilde{\kappa}_2$ scatter plot to evaluate how well low backscatter regions of various origin are separated. The results are presented separately for the two geographical regions.

4.1. North Sea and Barents Sea

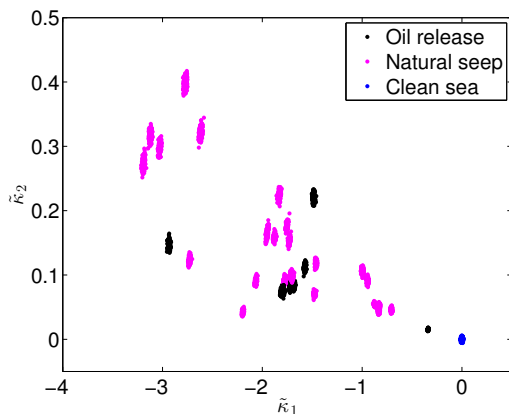
Fig. 2(a) shows the resulting scatter plot for the data collected in the North Sea and the Barents Sea. Each cluster contains 200 points and represents a given ROI. It can

be seen that the mineral oil releases are located close to each other, and mainly separated from the other region types. Natural phenomena of various types are located in different parts of the diagram. Simulated biogenic slicks (green) and one region assumed to be a low wind field (yellow) is located in the lower right part of the diagram. These regions have lower signal damping and lower texture compared to the mineral oil spills. The three yellow clusters located furthest to the left in the diagram is assumed to be thin ice, possibly mixed with calm open water. These regions produce a large signal damping and partly high texture.

Fig. 2(a) indicates that the normalized log-cumulants have potential for discrimination between anthropogenic oil releases and look-alikes of various origin. In [7], the possibility of drawing a decision boundary in the $\tilde{\kappa}_1 - \tilde{\kappa}_2$ space for classification of low backscatter regions were discussed. It was concluded that a large data set, with varying environmental, sensor and slick properties, is needed in order to define such a boundary. The results here presented show that for areas where thin ice is a possible look-alike, a more complex decision boundary is called for.



(a) North Sea and Barents Sea.



(b) Gulf of Mexico

Figure 2: $\tilde{\kappa}_1 - \tilde{\kappa}_2$ scatter plots.

4.2. Gulf of Mexico

The resulting $\tilde{\kappa}_1 - \tilde{\kappa}_2$ scatter plot for the Gulf of Mexico scenes is given in Fig. 2(b). Whereas the natural seeps are spread out over a large range of values, the man-made releases are more closely collected. The large spread of the natural seeps in the log-cumulant diagram can be due to varying age and slick properties. Also, many of these regions have complex shapes, and it was therefore more challenging to obtain an accurate segmentation. This could affect the resulting log-cumulant values.

It can be seen from Fig. 2(b) that the log-cumulant values for natural seeps and man-made oil releases overlap. These results suggest discrimination between anthropogenic oil releases and natural seeps may not be possible using $\tilde{\kappa}_1$ and $\tilde{\kappa}_2$ only. It should be mentioned that the slicks from the DWH spill may have properties similar to the natural seeps, as the former is also a release from the ocean bottom.

Note that, the Gulf of Mexico oil releases, both from the DWH accident and from ships, are located in the same part of the $\tilde{\kappa}_1 - \tilde{\kappa}_2$ diagram as the mineral oil spills in the North Sea/Barents Sea case.

4.3. Incidence Angle

At high incidence angles, the signal values can approach, and fall below, the sensor noise floor. In this case, the contrast to clean sea may be reduced, increasing the value of $\tilde{\kappa}_1$. Also, internal variations may not be detectable to the same extent, reducing the values of $\tilde{\kappa}_2$. Hence, the log-cumulants may only be useful in a limited range of incidence angles. In Fig. 2, all the available data are included, independent of incidence angle. In Fig. 3, only regions from scenes with $\theta \leq 40^\circ$ are shown. It can be seen that some of the regions in the lower right part of the diagrams are removed. For the North Sea/Barents Sea case a more clear separation between mineral oil spills and other phenomena is now observed. For the Gulf of Mexico, the man-made spills and natural seeps are still overlapping.

For future work, the incidence angle threshold should be investigated more carefully, and possibly a threshold must be set on the noise properties rather than on the incidence angle.

5. CONCLUSIONS AND FUTURE WORK

We show how the combination of first and second order log-cumulants may be useful for discrimination between some types of low backscatter ocean regions. In the North Sea/Barents Sea case, mineral oil releases are separated from simulated biogenic slicks and natural phenomena including low wind regions and thin ice. The method may not be suitable for data acquired at high incidence angles

due to noise effects. Results from the Gulf of Mexico indicate that natural seeps can not be distinguished from anthropogenic oil releases by using $\tilde{\kappa}_1$ and $\tilde{\kappa}_2$ only. The mineral oil releases from the two geographical regions have similar log-cumulant values.

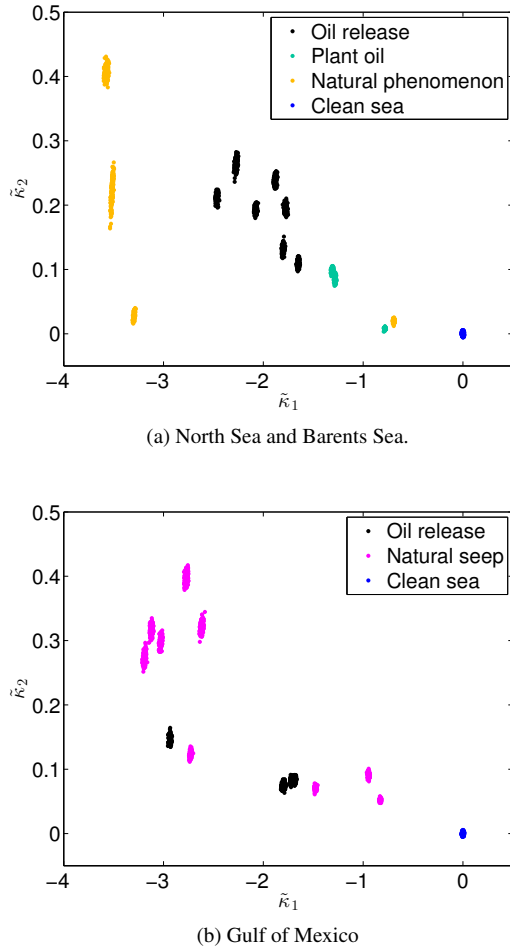


Figure 3: $\tilde{\kappa}_1 - \tilde{\kappa}_2$ scatter plots for scenes with $\theta \leq 40^\circ$.

Further work would include i) the collection of a more extensive data set (including ground truth information) for further testing and validation, ii) a more thorough investigation of the limitation on incidence angle or noise properties, iii) investigation of accurate segmentation methods, and iv) evaluation of the possibility to define classification rules in the $\tilde{\kappa}_1 - \tilde{\kappa}_2$ space as more data become available.

ACKNOWLEDGMENTS

The work is funded by the Research Council of Norway through the GlobOilRisk project under Grant 235444/O30. Radarsat-2 data are provided by NSC/KSAT under the Norwegian-Canadian Radarsat agreement 2010-2014. The authors would like to thank

NOFO for participation in the oil-on-water exercises, A.-B. Salberg at the Norwegian Computing Center for help with data collection, and A. P. Doulgeris at UiT-the Arctic University of Norway for participation in preliminary work.

REFERENCES

- [1] A. H. S. Solberg. Remote sensing of ocean oil-spill pollution. *Proc. IEEE*, 100(10):2931–2945, Oct. 2012.
- [2] C. Brekke and A. H. S. Solberg. Oil spill detection by satellite remote sensing. *Remote Sens. Environ.*, 95:1–13, 2005.
- [3] F. Nunziata, A. Gambardella, and M. Migliaccio. On the Mueller scattering matrix for SAR sea oil slick observation. *IEEE Geosci. Remote Sens. Lett.*, 5(4):691–695, Oct. 2008.
- [4] M. Migliaccio, F. Nunziata, and A. Gambardella. On the co-polarized phase difference for oil spill observation. *Int. J. Remote Sens.*, 30(6):1587–1602, Mar. 2009.
- [5] S. Skrunes, C. Brekke, and T. Eltoft. Characterization of marine surface slicks by Radarsat-2 multipolarization features. *IEEE Trans. Geosci. Remote Sens.*, 52(9):5302–5319, Sept. 2014.
- [6] S. Skrunes, C. Brekke, T. Eltoft, and V. Kudryavtsev. Comparing near coincident C- and X-band SAR acquisitions of marine oil spills. *IEEE Trans. Geosci. Remote Sens.*, 53(4):1958–1975, Apr. 2015.
- [7] S. Skrunes, C. Brekke, and A. P. Doulgeris. Characterization of low backscatter ocean features in dual-copolarization SAR using log-cumulants. *IEEE Geosci. Remote Sens. Lett.*, 12(4):836–840, Apr. 2015.
- [8] J.-M. Nicolas. Introduction aux statistiques de deuxième espèce: applications des logs-moments et des logs-cumulants à l’analyse des lois d’images radar. *Traitement du Signal*, 19(3):139–167, 2002.
- [9] J.-M. Nicolas and S. N. Anfinsen. Introduction to second kind statistics: Application of log-moments and log-cumulants to the analysis of radar image distributions. Translation from French of [8]. URL: <http://eo.uit.no/publications/jmn-trans-12.pdf>.
- [10] S. N. Anfinsen and T. Eltoft. Application of the matrix-variate Mellin transform to analysis of polarimetric radar images. *IEEE Trans. Geosci. Remote Sens.*, 49(6):2281–2295, Jun. 2011.
- [11] J.-S. Lee and E. Pottier. *Polarimetric Radar Imaging, from basics to applications*. CRC Press, Taylor and Francis Group, Boca Raton, USA, 2009.